

PHYSICOCHEMICAL PROBLEMS  
OF MATERIALS PROTECTION

Furan and Phenyl Substituted Triazolothiadiazine Derivatives  
as Copper Corrosion Inhibitors: Electrochemical and DFT Studies

Nasima Arshad<sup>a, \*, \*\*</sup>, Fouzia Altaf<sup>b</sup>, Muhammad Akram<sup>a</sup>, and Mehboob Ullah<sup>a</sup>

<sup>a</sup>Department of Chemistry, Allama Iqbal Open University, Islamabad, 44000 Pakistan

<sup>b</sup>Pakistan Council of Research in Water Resources, Ministry of Science and Technology, Islamabad, 44000 Pakistan

\*e-mail: nasimaa2006@yahoo.com

\*\*e-mail: nasima.arshad@aiou.edu.pk

Received May 15, 2018; revised January 2, 2019; accepted February 8, 2019

**Abstract**—This paper presents experimental aspects of two triazolodithiazine derivatives **1** {1-(6,7-di(furan-2-yl)-7H-[1,2,4]triazolo[3,4-b][1,3,4]thiadiazin-3-yl)ethanol} and **2** {6-phenyl-7H-[1,2,4]triazolo[3,4-b][1,3,4]thiadiazin-3-yl)ethanol} as copper corrosion inhibitors in borate (pH 8.4 and 10.4) aggressive media. Electrochemical findings by CV, polarization and EIS experiments were found inconsistent. The  $\eta\%$  values evaluated from all electrochemical methods were in good agreement and within the range of 93–97% at both pH. Compound **1** was found the most efficient corrosion inhibitor for Cu surface at pH 8.4 with inhibition efficiency upto 97%. Electrochemical responses and data interpretation confirmed that the process involved was charge transfer controlled and inhibitors were mixed type. Adsorption data was found best fit in Langmuir's adsorption isotherm and indicated spontaneity and stability of the compounds on Cu surface via physisorption. DFT computational studies further supported the experimental results.

**Keywords:** Cu corrosion, triazolodithiazine inhibitors, CV, potentiodynamic polarization, EIS, DFT

**DOI:** 10.1134/S2070205119040038

## 1. INTRODUCTION

Emerging industrial needs all over the world have several impacts on environment. Implication of various metals and their alloys in most of the industries could not be denied but their exposure to aggressive environments/media cause deterioration of their surfaces and as a result metal/alloy gets corroded [1]. Corrosion of a metal/alloy could be controlled by several methods like anodic/cathodic protection, painting, electroplating, galvanizing and the use of organic/inorganic inhibitors. Among them organic corrosion inhibitors were proven by several researcher to have excellent corrosion inhibitory efficiencies [2, 3]. Since metal corrosion is often an electrochemical process; redox behavior of metal surface in aggressive medium without and in the presence of a compound indicated about its effectiveness as corrosion inhibitor.

The ability of compound to protect a metal from corrosion depends on several factors such as film growth of the inhibitor by polymerization,  $\pi$ – $\pi$  and Van der Waals interactions, bonding strength with the metal's surface and the presence of oxygen, nitrogen and sulfur hetero atoms in its molecular structure. Moreover, number and type of atoms, bonding groups, temperature, pH and stability of aggressive

environments are the other factors that can affect corrosion inhibition efficiency of a compound [4–11].

Broader industrial and domestic applications of copper metal and its alloys are obvious as use in electric and electronic devices, marine industries, power stations, heat exchangers, cooling towers, pipelines etc [12, 13]. One of the major causes of copper corrosion in cooling towers and power plants is the usage of borate as a cooling agent [14]. The corrosion of copper and formation of corrosion products on its surface offer a negative effect on the performance of a system constructed from copper and may reduce its efficiency [15]. Extensive industrial utility of copper has attracted several researchers to work on the issue of its protection from corrosion.

The corrosion inhibition potential of heterocyclic compounds from the class of azoles, triazoles, benzimidazoles as well as Schiff bases have been reported for various metals and alloys [5, 16–18]. Triazolothiadiazine, another class of heterocyclic compounds, possess four nitrogen atoms and a sulfur atom along with a five member aromatic ring which is a  $\pi$  electron excessive system. These compounds have outstanding inhibition as compared to the compounds having only nitrogen atoms or sulfur atoms in their structures [19–21].

The present study was aimed to investigate the inhibitory and adsorption properties of furan and phenyl substituted triazolothiadiazine derivatives **1** and **2** for copper (in borate buffers of pH 8.4 and 10.4) by

Supplementary materials are available for this article at <https://doi.org/10.1134/S2070205119040038> and are accessible for authorized users.

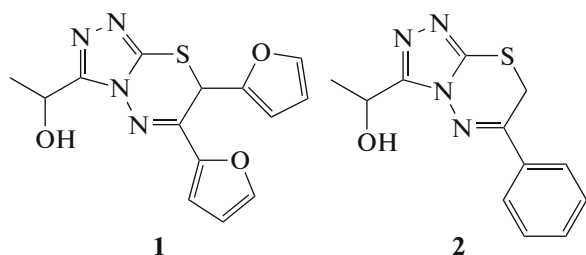


Fig. 1. Structures of investigated compounds.

electrochemical analysis. Investigated compounds are shown in Fig. 1 for their chemical structures.

## 2. EXPERIMENTAL

### 2.1. Surface Preparation

The chemical compositions of copper 10100 (in wt %) is 99.99%. The surfaces of Cu were chopped into circular discs in die cutting machine and disc was embedded in Teflon tubes with exposed surface area of 1 cm<sup>2</sup>. The surface of working electrode was made smooth by abrading with emery papers of different grit sizes (e.g. 350, 800, 1200, 1600, and 2500), degreased with acetone, ultrasonicated for 3 min, thoroughly rinsed with distilled water and finally dried in air. Each electrode was freshly prepared every time immediately before its use.

### 2.2. Chemicals and Solution Preparations

All chemicals and reagents used in experimental work were of analytical grade. Synthesis of furan and phenyl substituted triazolothiadiazine have been reported somewhere else [22]. Stock solutions ( $5.0 \times 10^{-3}$  M) of each compound was prepared separately and further diluted to various concentrations ranging from  $0.05 \times 10^{-3}$ – $0.25 \times 10^{-3}$  M. Borate buffers of pH 8.4 and 10.4 were prepared from orthoboric acid (H<sub>3</sub>BO<sub>3</sub>) and sodium tetraborate (Na<sub>2</sub>B<sub>4</sub>O<sub>7</sub> · 10H<sub>2</sub>O) and used as aggressive medium for copper corrosion.

### 2.3. Instrumentations

Electrochemical studies on Cu-surface were carried out by using electrochemical system “AUTOLAB” PGSTAT-302 potentiostat/galvanostat with GPES and FRA-2 modules and software package version 4.9 (Eco Chemie; Netherland). For cyclic voltammetry and potentiodynamic polarization measurements GPES module, while for impedance studies FRA-2 module was run separately. pH meter (Jenway; model 3510) was used to adjust required pH values of borate buffers.

### 2.4. Experimental Procedure

The sample solutions were taken in a single compartment double layer electrochemical cell (Mr. Bob's cell) which was attached to water circulator system for temperature control. 1 cm<sup>2</sup> Cu-disc in Teflon tube was used as working electrode along with reference SCE (saturated calomel electrode) and platinum wire counter electrode. The SCE was placed in a Lugging capillary and the tip was kept closer to the surface of the working electrode so that IR drop could be minimized. Firstly, voltammograms of bared Cu electrode in solution having pH 8.4 and 10.4 was recorded separately in potential range of 1 V to –1.2 V vs. SCE and then voltammetric responses in the presence of various concentrations of investigated compounds within same potential range were recorded at both pH. The potential scan rate was adjusted at 20 mV s<sup>-1</sup>. Before performing CV experiment, the surface of Cu electrode was immersed for some time in respective aggressive media (borate buffers of pH 8.4 and 10.4) in order to achieve a steady-state open circuit potential (OCP). Tafel regions of the polarization curves were directly obtained from CV responses in the absence and presence of compound's concentrations and potentiodynamic polarization data was obtained. Electrochemical impedance measurements were carried out at steady state OCP with amplitude of 10 mV ac sine wave by using FRA-2 module of the electrochemical system. The frequency range of 100 mHz – 100 mHz was used. Impedance spectra were recorded in the form of Nyquist and Bode plots for Cu without and in the presence of various concentrations of compounds. All experimental work was done at room temperature ( $25 \pm 0.5^\circ\text{C}$ ).

### 2.5. DFT Quantum Computational Calculations

Density functional theory (DFT) with Gaussian 03 software was employed to get optimized structures of the investigated corrosion inhibitors using the basis set, 3-21G\*. Becke three-parameter hybrid (B3) exchange functional in combination with the Lee–Yang–Parr (LYP) correlation functional (B3LYP) was used to determine the optimized geometries and all other computable properties.

## 3. RESULTS AND DISCUSSION

### 3.1. Cyclic Voltammetric Studies of Bare Copper Surface

Cyclic voltammograms of pure copper (99.99%) electrode were recorded in borate buffers at pH 8.4 and 10.4 and shown in Fig. S1 (in supporting information). These voltammograms showed strong oxidation and reduction peaks within the potential range of 1 V to –1.2 V vs. SCE. One broader oxidation peak appeared in the voltammogram that was assigned to two oxidation peaks due to electro-formation of Cu<sub>2</sub>O first and then formation of CuO. A broader shoulder

appeared over an extended potential range showed the formation of  $\text{Cu}(\text{OH})_2$ . While, two separate cathodic peaks at more negative potential range showed reduction of  $\text{CuO}$  into  $\text{Cu}_2\text{O}$  first and then  $\text{Cu}_2\text{O}$  into  $\text{Cu}$  [5, 9]. Shift in the anodic peak towards more positive potential was observed at pH 8.4 ascribing difficulty in the oxidation of  $\text{Cu}$  at low pH. The cathodic peak also showed an anodic shift at pH 8.4 which indicated easier reduction of  $\text{CuO}$  and  $\text{Cu}_2\text{O}$  at this pH. Decrease in both cathodic and anodic peak currents at pH 8.4 further indicated slow charge transfer process at low pH. The electrochemical behavior of  $\text{Cu}$  ascribed that oxidation process was thermodynamically more feasible and kinetically faster with the increase in pH.

### 3.2. Cyclic Voltammetric Studies of Cu – Compound Interaction

CV responses were recorded separately for  $\text{Cu}$  electrode in the presence of different concentrations ( $0.05 \times 10^{-3}$ – $0.25 \times 10^{-3}$  M) of **1** and **2** and shown in Fig. 2. The observed decreasing trend for both cathodic and anodic peaks of corroded  $\text{Cu}$  surface confirmed that the surface of  $\text{Cu}$  was affected by inhibitor's concentrations. The decrease in current densities of anodic peaks indicated the sluggishness of the corrosion process in the presence of inhibitors at both pH, while the decrease in current densities for the two cathodic peaks inferred a significant adsorption of compound on  $\text{Cu}$  surface. These changes in the current densities may be related to less availability of  $\text{Cu}$  sites for oxidation and reduction processes as blocked by adsorbed inhibitor molecules; hence decreasing the corrosion. A very slow corrosion process, still in the presence of inhibitor, may be indicative of presence of some defective sites where redox activity of  $\text{Cu}$  may occur [23]. The decrease in the corrosion current densities was observed maximum with the optimum concentration of  $0.25 \times 10^{-3}$  M. However, maximum suppression in both cathodic and anodic peaks was observed with compound **1** which is indicative of comparatively strong interaction of this compound with the metal surface via adsorption.

Anodic peak data before and after the addition of inhibitor concentrations was further used to determine the corrosion inhibition efficiency. Anodic peak was preferably considered because it was symmetric and showed regular peak current values. The values of percent inhibition efficiency were evaluated using the following equation and given in Table 1

$$\eta\% = 100 \times \left[ 1 - \frac{(I_a)_i}{(I_a)_o} \right]. \quad (1)$$

Where,  $(I_a)_o$  and  $(I_a)_i$  are current densities of copper in the absence and presence of inhibitor's concentrations, respectively. The surface coverage parameter

**Table 1.** Surface coverage and inhibition efficiency for  $\text{Cu}$  surface in the presence of **1** and **2** at pH 8.4 and 10.4

pH	Inhibitor conc., $10^{-3}$ M	<b>1</b>		<b>2</b>	
		( $\theta$ )	$\eta\%$	( $\theta$ )	$\eta\%$
8.4	0.05	0.31	31	0.29	29
	0.1	0.58	58	0.53	53
	0.15	0.71	71	0.68	68
	0.2	0.87	87	0.83	83
	0.25	0.97	97	0.96	96
10.4	0.05	0.28	28	0.27	27
	0.1	0.50	50	0.48	48
	0.15	0.67	67	0.64	64
	0.2	0.82	82	0.79	79
	0.25	0.96	96	0.94	94

( $\theta$ ) corresponds to one hundredth of the percent efficiency  $\left[ 1 - \frac{(I_a)_i}{(I_a)_o} \right]$ .

The surface coverage values of both inhibitors were evaluated maximum at moderately alkaline medium (pH 8.4), Table 1. At high alkaline medium (pH 10.4 and above) corrosion rate is faster due to the formation of more dense and thick film of monoclinic copper oxide ( $\text{CuO}$ ). Despite the fact, that the donor ability of the compound towards metal surface would be greater at higher pH; the adsorption of inhibitor molecules is comparatively less feasible at pH 10.4 as the thickness of  $\text{CuO}$  film goes on increasing with increase alkalinity. In contrast, at pH 8.4, very thin and smooth layer of  $\text{Cu}_2\text{O}$  is formed at the electrode surface and interaction of compound via adsorption is more feasible at pH 8.4 than at 10.4 [24].

The inhibition efficiencies of both compounds were evaluated >90% at their maximum optimized concentration. However, compound **1** showed slightly greater inhibition (97% at pH 8.4 and 96% at pH 10.4) than the compound **2**. A comparatively better inhibition of **1** than **2** may be attributed to presence of three hetero atoms (N, S and O) in the **1** structure as compared to **2** where only N and S are present which could be comparatively more favorable for the protection of a metal surface from corrosion.

### 3.3. Potentiodynamic Polarization Measurements

Potentiodynamic polarization is one of the informative methods to envisage corrosion mechanism, corrosion kinetics and material (metal/metallic alloy) susceptibility towards corrosion in specific designed environment.

The potentiodynamic polarization curve of  $\text{Cu}$  at pH 8.4 containing different concentrations of investi-

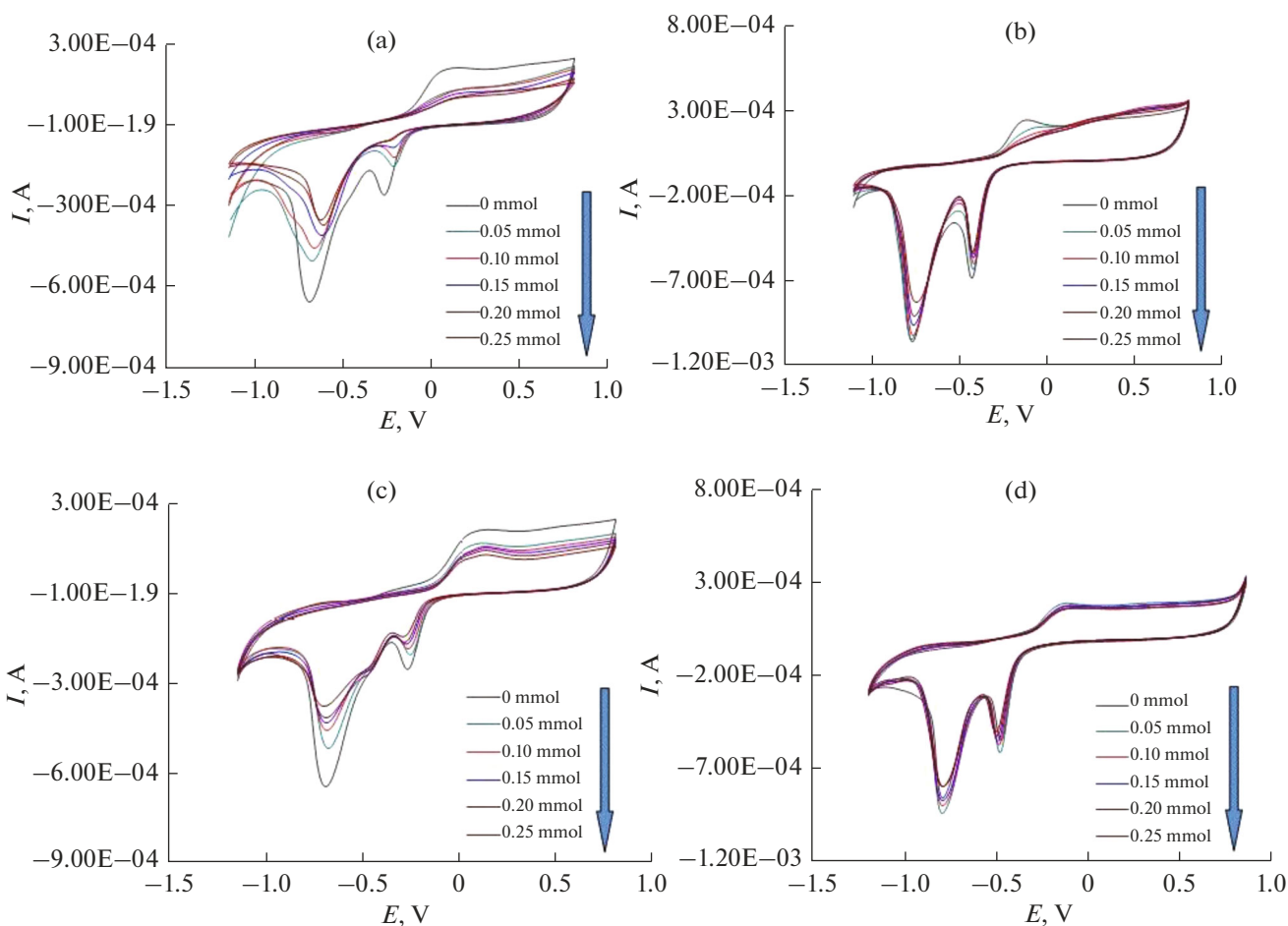


Fig. 2. CV of Cu surface in the absence and presence different conc. of **1** (top) and **2** (bottom) at pH 8.4 (left side) and 10.4 (right side).

gated compound is shown in Fig. 3. Potentiodynamic parameters including  $C_R$  (corrosion rate),  $I_{corr}$  (corrosion current density),  $R_p$  (polarization resistance),  $\beta_c$  and  $\beta_a$  (cathodic and anodic Tafel slopes) were evalu-

ated from extrapolation of Tafel plots and the values are given in Table 2. The inhibitor efficiency was calculated using the following equation:

$$\eta\% = 100 \times \left[ \frac{(R_p)_i - (R_p)_o}{(R_p)_i} \right], \quad (2)$$

where,  $(R_p)_o$  and  $(R_p)_i$  are polarization resistance in the absence and presence of the inhibitor' concentrations, respectively. The weight loss ( $W \text{ gm}^{-2} \text{ h}^{-1}$ ) was calculated theoretically using following equation [25]:

$$W = \frac{I_{corr} t M}{F} \times 10^4, \quad (3)$$

where,  $I_{corr}$ ,  $t$ ,  $M$  and  $F$  are the corrosion current density ( $\text{A cm}^{-2}$ ), time (s), equivalent molar weight of copper ( $\text{g mol}^{-1}$ ) and Faraday constant ( $96500 \text{ C mol}^{-1}$ ), respectively, while a constant value of  $10^4$  is multiplied for unit conversion from  $\text{cm}^2$  to  $\text{m}^2$ .

The results given in Table 2 showed slightly rise in the values of anodic ( $\beta_a$ ) and cathodic ( $\beta_c$ ) Tafel slopes, increase in polarization resistance ( $R_p$ ), change in  $E_{corr}$  to more negative values and decreases in  $I_{corr}$

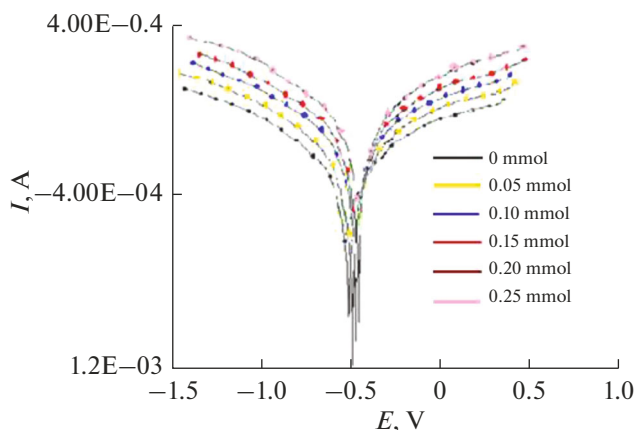


Fig. 3. Potentiodynamic polarization curves for Cu surface at pH 8.4 in the presence of different concentrations of **1**.

**Table 2.** Polarization parameters of Cu surface in the absence and presence of various concentrations of **1** and **2** at pH 8.4 and 10.4

Cu-Inhibitor	pH	Conc., 10 <sup>-3</sup> M	$I_{\text{corr}} \times 10^{-5}$ , A cm <sup>2</sup>	$R_p \times 10^3$ , $\Omega$ cm <sup>2</sup>	$E_{\text{corr}}$ , V	$\beta_c$ , V dec <sup>-1</sup>	$\beta_a$ , V dec <sup>-1</sup>	$\eta\%$	$W \times 10^{-3}$ , g m <sup>-2</sup> h <sup>-1</sup>	Corro.rate , mm/year
Cu-1	8.4	0.00	7.267	5.843	-0.572	0.483	0.307	—	1.43	0.194
		0.05	5.140	8.270	-0.551	0.475	0.312	30	1.01	0.177
		0.1	3.234	13.620	-0.545	0.461	0.303	57	0.63	0.158
		0.15	2.164	19.890	-0.523	0.456	0.301	71	0.43	0.129
		0.2	1.039	42.210	-0.519	0.447	0.361	86	0.21	0.110
		0.25	0.268	130.700	-0.504	0.433	0.308	96	0.06	0.079
Cu-2	8.4	0.00	7.267	5.843	-0.572	0.483	0.307	—	1.43	0.194
		0.05	5.204	8.148	-0.560	0.418	0.366	29	1.03	0.172
		0.1	3.577	12.300	-0.557	0.448	0.394	52	0.71	0.150
		0.15	2.554	16.910	-0.535	0.418	0.372	66	0.50	0.133
		0.2	1.301	32.250	-0.528	0.396	0.320	82	0.26	0.116
		0.25	0.396	110.380	-0.515	0.398	0.321	95	0.082	0.095
Cu-1	10.4	0.00	10.804	7.407	-0.505	0.433	0.266	—	2.13	0.152
		0.05	7.714	10.508	-0.485	0.382	0.239	29	1.52	0.097
		0.1	5.626	14.349	-0.461	0.367	0.230	48	1.11	0.061
		0.15	3.598	21.962	-0.446	0.350	0.227	66	0.71	0.052
		0.2	1.844	45.207	-0.421	0.325	0.217	83	0.36	0.330
		0.25	0.513	159.838	-0.401	0.302	0.212	95	0.10	0.024
Cu-2	10.4	0.00	10.804	7.407	-0.545	0.433	0.266	—	2.13	0.152
		0.05	7.886	10.251	-0.505	0.434	0.247	27	1.56	0.101
		0.1	5.878	13.895	-0.492	0.424	0.240	46	1.16	0.082
		0.15	3.800	20.867	-0.477	0.422	0.241	64	7.50	0.064
		0.2	2.156	37.819	-0.461	0.414	0.237	80	4.26	0.047
		0.25	0.752	112.92	-0.429	0.408	0.233	93	1.48	0.029

with inhibitor's concentrations. These changes in the parameters indicated that both anodic copper dissolution and cathodic reduction of copper were inhibited and suggested that the investigated compounds act as mixed type inhibitors.

The inhibition efficiencies evaluated from potentiodynamic parameters were also found >90% and in consistent with that obtained from CV results. The decrease in corrosion rate is more pronounced at pH 8.4 with both compounds, the reason is same as discussed in previous section.

### 3.4. Adsorption of Inhibitor on Pure Copper Surface

Corrosion inhibitory efficiency of a compound depends upon several factors including number of active sites at metal surface, size of inhibitor, charge density, metal–inhibitor interaction and complex formation [26]. The nature of the metal–inhibitor inter-

action or adsorption mechanism can be estimated from the experimental surface coverage ( $\theta$ ) data.

$$\text{The values of surface coverage, } \theta = \left[ 1 - \frac{(I_a)_i}{(I_a)_o} \right],$$

obtained from corrosion current densities of Cu before and after inhibitor's concentrations were subjected to different adsorption isotherms and was found to be well fitted with modified Langmuir adsorption isotherm (Eq. 4) as evident from linear regression ( $R^2$ ) values:

$$\frac{C_i}{\theta} = \frac{1}{K} + aC_i, \quad (4)$$

where,  $C_i$  is inhibitor's concentration. The plot of  $C_i/\theta$  versus  $C_i$  yielded a straight line ( $R^2 = 0.980, 0.978$  for **1** and  $0.994, 0.987$ , for **2** at pH 8.4 and 10.4, respectively) and provided in Fig. 4. The adsorption constant  $K_{\text{ads}}$  was evaluated from the reciprocal of the intercept.

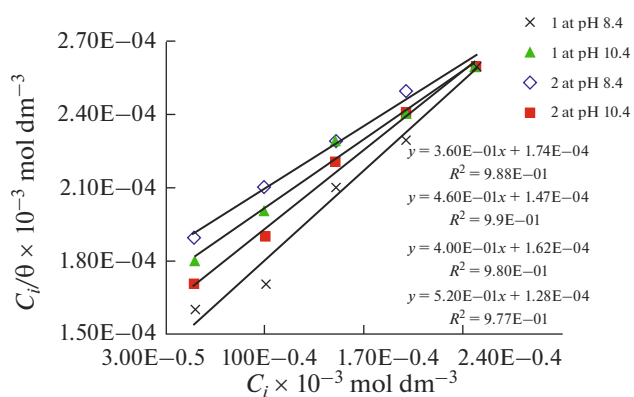


Fig. 4. Langmuir's isotherm for adsorption of compounds.

where,  $C_{\text{solvent}}$  is the molar concentration of the solvent which in case of water is  $55.5 \text{ mol/dm}^3$ . Adsorption data is provided in Table 3, which revealed greater  $K_{\text{ads}}$  values for the compound **1** at both pH. However, at pH 8.4, the  $K_{\text{ads}}$  value for **1** was evaluated comparatively

greater than that at pH 10.4.  $\Delta G_{\text{ads}}^\circ$  for both the compounds were evaluated negative and below  $-20 \text{ kJ/mol}$  and assured the spontaneity and stability of the compounds in the form of adsorbed layer on Cu– surface via physisorption [26]. Further, a dimensionless separation factor,  $R_L$ , was calculated by using following equation:

$$R_L = \frac{1}{1 + K_{\text{ads}}C_i} \quad (6)$$

The corresponding  $\Delta G_{\text{ads}}^\circ$  values were calculated from following equation:

$$K_{\text{ads}} = \frac{1}{C_{\text{solvent}}} \exp \left( \frac{-\Delta G_{\text{ads}}^\circ}{RT} \right), \quad (5)$$

$R_L$  values were evaluated lesser than 1 ( $R_L < 1$ ) which is a prerequisite for the favorable adsorption process [27]. Adsorption parameters indicated comparatively strong adsorption of **1** on Cu surface at pH 8.4 and the results showed consistency with electrochemical findings.

Table 3. Adsorption parameters calculated from Langmuir's adsorption isotherm

Inhibitor	pH	Conc., $10^{-3} \text{ M}$	$C_i/\theta$	$K_{\text{ads}}, \text{ M}^{-1}$	$\Delta G_{\text{ads}}^\circ, \text{ kJ/mol}$	$R_L$
<b>1</b>	8.4	0.00	—	7.812	-12.26	—
		0.05	0.16			0.72
		0.1	0.17			0.56
		0.15	0.21			0.46
		0.2	0.23			0.39
		0.25	0.26			0.34
<b>2</b>	8.4	0.00	—	6.802	-11.91	—
		0.05	0.17			0.75
		0.1	0.19			0.60
		0.15	0.22			0.49
		0.2	0.24			0.42
		0.25	0.26			0.37
<b>1</b>	10.4	0.00	—	5.747	-11.50	—
		0.05	0.18			0.78
		0.1	0.20			0.64
		0.15	0.23			0.54
		0.2	0.24			0.47
		0.25	0.26			0.41
<b>2</b>	10.4	0.00	—	6.172	-11.71	—
		0.05	0.19			0.76
		0.1	0.21			0.62
		0.15	0.23			0.52
		0.2	0.25			0.45
		0.25	0.26			0.39

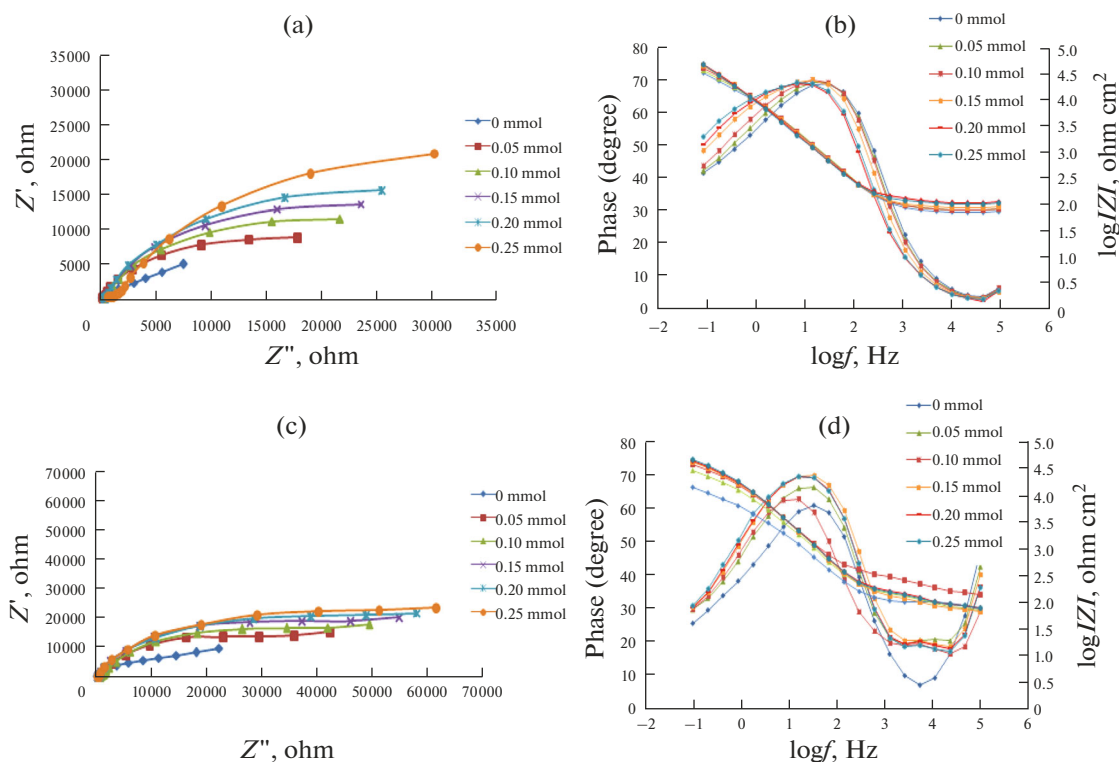


**Fig. 5.** Nyquist (left) and Bode (right) plots of Cu-surface at OCP in the absence and presence of various concentrations of compounds; **1** (top) and **2** (bottom) at pH 8.4.

### 3.5. Electrochemical Impedance Spectral Interpretation of Cu–Compound Interaction

EIS has successfully been employed to study the corrosion kinetics and to understand the mechanism of inhibitory activity of compounds on corrode metal surface. Impedance data is based on modeling a corrosion process by an electrical circuit. The inhibitory effect of investigated compounds **1** and **2** on electrochemical process of Cu surface was studied at open circuit potential (OCP) using EIS technique.

Impedance spectra of Cu–electrode in the absence and presence of inhibitors at pH 8.4 are shown in Fig. 5 in the form of Nyquist and Bode plots and at pH 10.4 in Fig. S2 (in supporting information). Nyquist plots showed that with the increase in inhibitor's concentration the diameter of semicircle increased significantly which indicated that the resistance of Cu– surface for the charge transfer after adsorption of inhibitor molecule has increased [28]. Bode plots showed that both capacitive and low frequency resistive regions of impedance shifted to higher values with increasing inhibitor's concentration which corresponded to the dominance of the resistive behavior of Cu surface in the presence of inhibitor.

### 3.6. Open Circuit Topology and EIS Measurements

Impedance data fitting into an equivalent circuit model provides basis in the physical electrochemistry of the system. The circuit topology fit in for experimental impedance data in present studies was proposed as;  $R_s(R_1Q_1[R_2Q_2])$ . This topology corresponded to corroding metal (Cu) coated with inhibitor in borate buffer and shown in Fig. 6. In the proposed topology;  $R_s$  indicated resistance of solution,  $R_1-Q_1$  (high frequency circuit) represented capacitance and resistance of the surface film most likely a compact oxide layer while  $R_2-Q_2$  (medium frequency circuit) corresponded to double layer capacitance and charge transfer resistance.

The sign of  $Q$  showed the possibility of a non-ideal capacitance called CPE (constant phase element) with varying values of  $n$ . Further, literature revealed that theoretical agreement with the experimental data could be achieved by introducing frequency dependent CPE instead of pure capacitance and Warburg impedance [29]. CPE is a non- instinctive circuit element, while in real system some distribution/or dispersion of the value of some physical property may occur. The coefficient ( $n$ ) represents the depressed feature of the capacitive loop in Nyquist Plot. Depression in the semicircle usually arises due to the fre-

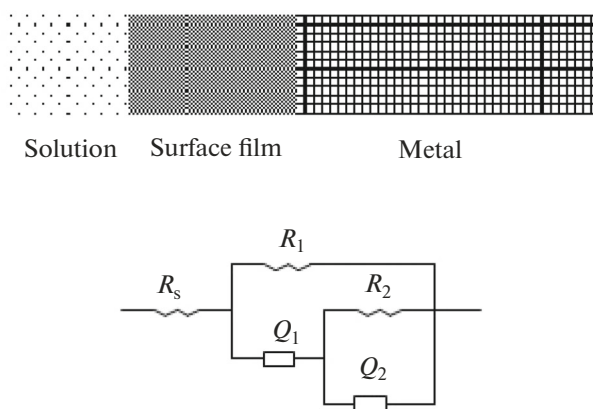


Fig. 6. Proposed equivalent circuit topology.

quency dispersion if the metal surface is rough and inhomogenized [30, 31].

The experimental data in present studies was found better fit with the theoretical data using frequency dependant CPE. The impedance of constant phase element is given by the following equation [8, 30, 31]:

$$Z_{CPE} = A^{-1} (I\omega)^{-n}, \quad (7)$$

where,  $A$ ,  $\omega$ , and  $I$  are CPE constant, angular frequency ( $\text{rad s}^{-1}$ ) and imaginary number ( $i^2 = -1$ ) respectively, while exponent  $n$  is used for measuring roughness and inhomogeneity of the metal surface. CPE behavior could be manifested as an analogous in the frequency domain. Depending upon the value of  $n$ , CPE represents different components of the circuit i.e., resistance ( $n = 0, A = R$ ), capacitance ( $n = 1, A = C$ ), inductance ( $n = -1, A = L$ ) or Warburg impedance ( $n = 0.5, A$ ). The greater value of exponent  $n$  portray smoothness and high surface homogeneity, while small value of  $n$  showed surface porosity which permits ions or solvent.

The fit parameters obtained for Cu–surface before and in the presence of various concentrations of investigated inhibitors are given in Table 4. Tabulated data shows that the value of  $R_1$  (charge transfer resistance) increased as inhibitor's concentration increased. The rise in  $R_1$  values with inhibitor's concentration could be assigned to decrease in the corrosion rate. Decrease in the value of  $Q_1$  (double layer capacitance) with inhibitor's concentration further revealed that the inhibitor molecules get adsorb on metal surface by preventing the charge species to reach to the metal surface. Similarly increase in the value of  $R_2$  (resistance of adsorb inhibitor) and decrease in the values of  $Q_2$  (capacitance of metal after adsorb layer of inhibitor) with increasing inhibitor's concentration, as observed in present studies, were indicative of formation of adsorbed layer of inhibitor molecules by making the charge transfer process very sluggish and decrease in the corrosion rate, respectively.

The value of  $n_1$  at the beginning was found high and then slightly decreased as inhibitor concentration increased. This decrease in  $n_1$  value was suggestive of formation of heterogeneous film at the surface of metal. The  $n_2$  value increased with inhibitor concentration which indicated that redox process at low frequencies was not due to diffusion or the reduction of dissolved oxygen but inhibitor molecules get accumulated at the surface of electrode.

Increase in the values of  $R_1$  and  $R_2$  and  $n_2$  while decrease in  $Q_1$  and  $Q_2$  were found more pronounced for the compound **1** than **2** at pH 8.4. Comparatively greater inhibitory effect of **1** could further be rationalized due to the presence of three hetero atoms in the structure as discuss in earlier section.

### 3.7. Determination of Inhibitor's Efficiency

The total resistance ( $R_T$ ) at the interface of metal and solution is the sum of  $R_1$  (charge transfer resistance) and  $R_2$  (faradic resistance) i.e., ( $R_T = R_1 + R_2$ ) and generally related to the corrosion rate [9, 23]. Increase in  $R_T$  in the presence of inhibitor concentration indicated resistance of that inhibitor for electron transfer. Using the values of total resistance ( $R_T = R_1 + R_2$ ) in following equation, inhibition efficiency of investigated compounds for the Cu–surface can be calculated as;

$$\eta(\%) = \left[ \frac{(R_T)_i - (R_T)_0}{(R_T)_i} \right] \times 100. \quad (8)$$

The subscripts 'i' and 'o' for  $R_T$  are used for total resistance with and without inhibitor, respectively. The calculated values are provided in Table 4.

Data showed that  $\eta\%$  was markedly increased with inhibitor's concentration. However, at higher concentrations (after  $0.2 \times 10^{-3}$  M) this rise in  $\eta\%$  was less pronounced. This could be explained on the basis of free Cu–surface which was initially available for the adsorption of inhibitor molecules and afterwards, at higher inhibitor's concentration, no free surface was further available to the molecules to be adsorbed, hence decreasing the rate of adsorption. The % inhibition evaluated from impedance, CV and polarization have shown the same trends in values.  $\eta\%$  calculated from all electrochemical methods revealed compound **1** as comparatively better corrosion inhibitor than **2**. However, both compounds showed >90% inhibition efficiencies at both pH.

It may also be mentioned that inhibition efficiencies lie in the range of 93–97% at both pH indicating **1** and **2** as excellent inhibitors as compare to our previously reported inhibitors from the same classification {1-(6-(4-nitrophenyl)-7H [1, 2, 4]triazolo[3,4-b], [1, 3, 4]thiadiazine3-yl)ethanol (NTTD) and 6-phenyl-3-(trifluoromethyl)-7H-[1, 2, 4]triazole[3,4-b]thiadiazine (FTTD)} where only compound FTTD



**Table 4.** Impedance parameters for Cu in the absence and presence of inhibitor's concentrations at pH 8.4 and 10.4

Inhibitor	pH	Conc., 10 <sup>-3</sup> M	$R_1 \times 10^3$ , $\Omega \text{ cm}^2$	$Q_1 \times 10^{-4}$ , $\text{F cm}^{-2} \text{ s}^{1-n}$	$n_1$	$R_2 \times 10^3$ , $\Omega \text{ cm}^2$	$Q_2 \times 10^{-4}$ , $\text{F cm}^{-2} \text{ s}^{1-n}$	$n_2$	$R_T \times 10^3$ , $\Omega \text{ cm}^2$	$\eta$
<b>1</b>	8.4	0.00	6.75	157.23	0.786	2.95	180.32	0.543	9.7	–
		0.05	9.12	115.32	0.792	4.65	155.02	0.553	13.77	29
		0.10	15.36	98.37	0.788	7.38	136.22	0.567	22.74	57
		0.15	22.18	79.38	0.784	10.65	114.32	0.582	32.83	70
		0.20	55.98	62.99	0.779	19.92	99.64	0.588	75.9	87
		0.25	118.45	55.82	0.761	68.87	75.34	0.591	187.32	95
<b>2</b>	8.4	0.00	6.75	157.23	0.786	2.95	180.32	0.543	9.7	–
		0.05	8.15	130.44	0.781	5.31	161.12	0.549	13.46	28
		0.10	13.22	101.29	0.778	6.7	143.09	0.552	19.92	51
		0.15	20.33	86.01	0.77	9.27	121.11	0.55	29.6	67
		0.20	44.61	71.94	0.768	16.02	108.05	0.571	60.63	84
		0.25	101.75	59.38	0.763	59.74	82.66	0.585	161.49	94
<b>1</b>	10.4	0.00	8.99	75.32	0.770	3.74	1502.14	0.733	12.73	–
		0.05	9.71	62.1	0.754	8.63	743.16	0.791	18.34	31
		0.10	11.60	49.41	0.698	14.33	629.47	0.820	25.93	51
		0.15	15.32	36.84	0.678	24.65	435.32	0.831	39.95	68
		0.20	29.31	28.06	0.683	54.67	256.89	0.853	83.97	85
		0.25	65.70	21.89	0.675	88.67	101.65	0.874	154.35	95
<b>2</b>	10.4	0.00	8.99	75.32	0.77	3.74	1502.14	0.733	12.73	–
		0.05	9.6	69.19	0.764	7.99	951.2	0.751	17.59	28
		0.10	10.3	57.14	0.746	12.75	784.62	0.762	23.05	45
		0.15	13.56	43.12	0.715	22.61	596.31	0.796	36.17	65
		0.20	26.84	34.11	0.698	53.15	357.84	0.812	79.99	84
		0.25	70.95	25.93	0.684	112.63	215.62	0.843	183.58	93

has shown maximum inhibition efficiency of 86.53% at pH 8.4 [19].

### 3.8. Quantum DFT Studies

The optimized geometries of investigated compounds and their frontier molecular orbitals (HOMO and LUMO) are given in Fig. 7 and the computed parameters are provided in Table 5. The molecular reactivity depends on HOMO–LUMO distribution, where former is associated with the electron donating ability of a molecule and later indicates its ability to accept the electrons.

HOMO energy for **1** (–0.20 eV) was found comparatively high than that of **2** which showed more ability of **1** to donate electrons. Similarly, HOMO–LUMO gap is an important stability index that helps to predict the inhibition efficiency [32]. In present studies it was found least ( $\Delta E = 0.13$  eV) for compound **1** attributing its comparatively better inhibition efficiency than **2**. Further, HOMO density is higher in the zone near to the thiadiazine ring and prominent on furan rings;

hence the preferred active sites for donating electrons in **1** are mainly located within the region around sulfur, oxygen, nitrogen and  $\pi$ -electrons. From HOMO and LUMO diagrams it could be assumed that the triazole, thiadiazine and furan rings in **1** act as main sites to donate electrons. As a result coordinate bond with un-occupied  $d$ -orbitals of Cu may be formed. On the other hand, C–C bonds may act as dominant sites to accept electrons from  $d$ -orbitals to form back-donating bond. Furthermore, lower value of global hardness, higher value of dipole moment and fraction of electron transferred were evaluated for **1** ( $\gamma$ ; 0.07,  $D$ ; 6.57,  $\Delta N$ ; 5.6/0.14) and attributed to the presence of two more five member furan groups that may enhance inhibition efficiency of **1** as compared to **2** [33].

## 4. CONCLUSIONS

Taking a perspective view on Cu corrosion protection by triazolothiadiazine derivatives, present studies could be summarized as follows:

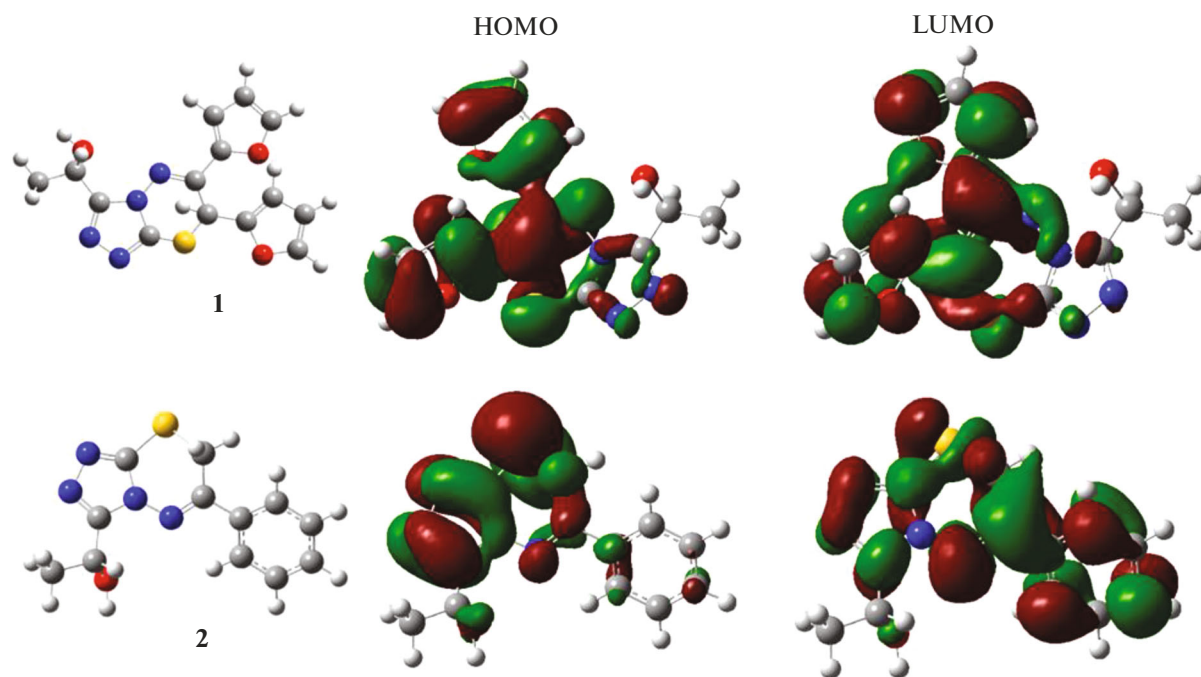


Fig. 7. DFT/B3LYP/6-31G\* optimized geometries of **1** and **2** derivatives and their frontier molecular orbitals.

- Electrochemical mechanisms for Cu corrosion in moderately and strongly alkaline medium are different due to the formation of dense monoclinic layer of CuO at pH 10.4 and a smooth thin layer of Cu<sub>2</sub>O at pH 8.4.

- Measurements of peak current in CV experiments and circuit elements ( $R_s$ ,  $R_1$ ,  $R_2$ ,  $Q_1$ ,  $Q_2$ ) in EIS experiments calculated from regression calculation revealed comparatively better inhibition at low pH.

- In the presence of **1** and **2**, decline in the Cu corrosion rates were evaluated from 0.194 to 0.079,

0.095 mm/year respectively at pH 8.4 and from 0.152 to 0.024, 0.029 mm/year, respectively, at pH 10.4, which is a significant decrease.

- EIS studies indicated that electrochemical processes in surface protection by inhibitors were charge transfer-controlled.

- Adsorption parameters  $K$ ,  $\Delta G_{\text{ads}}^\circ$  and  $R_L$  inferred the involvement of spontaneous and stable physisorption of the compounds on Cu surface in borate media.

- The % inhibition efficiencies evaluated from CV, potentiodynamic polarization and EIS showed same trends and consistency in results, although the three electrochemical methods have provided information about different aspects of the corrosion phenomena.

- Inhibitor efficiency (at saturation level) was evaluated greatest (upto 97%) for **1** at pH 8.4 and led to more feasible adsorption of inhibitor **1** with larger number of hetro-atoms in moderately alkaline media.

- Experimental results were justified from theoretical quantum investigations.

**Table 5.** Quantum-chemical parameters of the investigated corrosion inhibitors computed with DFT at B3LYP/6-31G\* level

Computational parameters	<b>1</b>	<b>2</b>
$E_{\text{HOMO}}$ , eV	-0.20	-0.24
$E_{\text{LUMO}}$ , eV	-0.07	-0.08
$\Delta E = E_{\text{LUMO}} - E_{\text{HOMO}}$ , eV	0.13	0.16
Ionization potential, eV	0.20	0.24
Electron affinity, eV	0.07	0.08
Binding energy, ka.u	-1.38	-1.16
Dipole moment, D	6.57	7.94
Electronegativity X	1.40	0.16
Global hardness $\gamma$	0.07	0.08
$\Delta N =$ Fraction of electron transfer (Fe)	5.6/0.14	6.84/0.16

#### ACKNOWLEDGMENTS

Authors are thankful to Dr. Uzma Yunus, Chemistry Department AIUO for donating compounds for corrosion studies.

## DISCLOSURE STATEMENT

The authors would like to declare that there is no any established conflict of interest.

## ASSOCIATED CONTENT

*Supporting Information*

Figures S1, S2; as supporting information for this study.

## REFERENCES

1. Fouada, A.S., Gouda, M.M., and Abd El-Rahman, S.I., *Chem. Pharm. Bull.*, 2000, vol. 48, p. 636.
2. Mojtaba, N., Mahmoud, Z., and J. Behroz, *Prot. Met. Phys. Chem. Surf.*, 2015, vol. 51, p. 285.
3. Mihajlović, M.B.P. and Antonijević, M.M., *Int. J. Electrochem. Sci.*, 2015, vol. 10, p. 1027.
4. Ramesh, S. and Rajeswari, S., *Corros. Sci.*, 2005, vol. 47, p. 151.
5. Altaf, F., Qureshi, R., Ahmed, S., Khan, A.Y., and Naseer, A., *J. Electroanal. Chem.*, 2010, vol. 642, p. 98.
6. Ameh, P.O. and Eddy, N.O., *Res. Chem. Intermed.*, 2014, vol. 40, p. 2641.
7. Eddy, N.O., Ameh, P.O., Gimba, C.E., and Ebenso, E.E., *J. Chem.*, 2013, vol. 2013, p. 10.
8. Eddy, N.O., *J. Adv. Res.*, 2011, vol. 2, p. 35.
9. Elayyoubi, S.B., Hammouti, S., Kertit, H.O., and Maarouf, E.B., *Rev. Met. Paris*, 2004, vol. 2, p. 153.
10. Okafor, P.C., Osabor, V., and Ebenso, E.E., *Pigm. Resin Technol.*, 2007, vol. 36, p. 299.
11. Bilgic, L. and Caliskan, N., *J. Appl. Electrochem.*, 2001, vol. 52, p. 79.
12. Duran, B., Bereket, G., and Duran, M., *Prog. Org. Coat.*, 2012, vol. 73, p. 162.
13. Sherif, S.M., Erasmus, R.M., and Comins J.D., *J. Colloid Interface Sci.*, 2007, vol. 309, p. 470.
14. Attia, A.A., Elmelegy, E.M., and Ahmed, M.A.B., *Asian J. Chem.*, 2016, vol. 28, p.267.
15. Altaf, F., Qureshi, R., and Ahmad, S., *J. Electroanal. Chem.*, 2011, vol. 659, p. 134.
16. Kim, Y.S., Kim, S.H., and Kim, J.G., *Met. Mater. Int.*, 2015, vol. 21, p. 1013.
17. Emergull, K.C., Kurtaran, R., and Atakol, O., *J. Corros. Sci.*, 2003, vol. 45, p. 2803.
18. Li, X., Deng, S., Fu, H., and Li, T., *Electrochim. Acta*, 2009, vol. 54, p. 4089.
19. Arshad, N., Akram, A.R., Akram, M., and Rasheed, I., *Prot. Met. Phys. Chem. Surf.*, 2017, vol. 53, p. 343.
20. Hussin, M.H. and Kassim, M.J., *J. Phys. Sci.*, 2010, vol. 21, p. 1.
21. Benali, O., Lerabi, I., Traisne, L.M., Gengembra, L., and Harek, Y., *Appl. Surf. Sci.*, 2007, vol. 253, p. 6130.
22. Yunus, U., Ahmed, S., Chahkandi, M., Bhatti, M.H., and Tahir, M.N., *J. Mol. Struct.*, 2017, vol. 1130, p. 688.
23. Bentiss, F., Lagrenée, M., Elmehdi, B., Mernari, B., Traisnel, M., and Vezin, H., *Corrosion*, 2002, vol. 58, p. 399.
24. Hukovic, M.M., Babic, R., and Paic, I., *J. Appl. Electrochem.*, 2000, vol. 30, p. 617.
25. Solmaz, R., *Corros. Sci.*, 2014, vol. 79, p. 169.
26. Saji, V.S., *Corros. Sci.*, 2010, vol. 2, p. 6.
27. Muhammad, T.A., Abdul Rahman, A.A., and Muhammad, S., *Sustainability*, 2015, vol. 7, p. 15302.
28. Hukovic, M.M., Babic, R., and Grubac, Z., *J. Appl. Electrochem.*, 2002, vol. 32, p. 35.
29. Amin, M.A., *J. Appl. Electrochem.*, 2006, vol. 36, p. 215.
30. Bentiss, F., Lagrenee, M., Traisnel, M., and Hornes, J.C., *Corros. Sci.*, 1999, vol. 41, p. 789.
31. Bentiss, F., Lagrenee, M., Traisnel, M., and Hornes, J.C., *Corros. Sci.*, 2005, vol. 47, p. 2915.
32. Belkheir, A.H., Ali, D., Mohammed, B., Hassan, Z., Said, B., and Salem, A.D., *J. Saudi Chem. Soc.*, 2014, vol. 5, p. 450.
33. Spirtovic-Halilovic, S., Salihovic, M., Veljovic, E., Osmanovi, C.A., Trifunovic, S., and Završnik, D., *Bull. Chem. Technol.*, 2014, vol. 42, p. 31.